IOP Publishing Physica Scripta
Phys. Scr. 95 (2020) 045602 (9pp) https://doi.org/10.1088/1402-4896/ab5d5a

# Effect of cross-focusing of two laser beams on THz radiation in graphite nanoparticles with density ripple

**Vishal Thakur**[1], **Niti Kant**[1] and **Shivani Vij**[2]

[1] Department of Physics, Lovely Professional University, G.T. Road, Phagwara 144411, Punjab, India
[2] Department of Applied Sciences, DAV Institute of Engineering & Technology, Jalandhar-144008, India

E-mail: svij25@yahoo.co.in

Received 14 August 2019, revised 10 November 2019
Accepted for publication 29 November 2019
Published 12 February 2020

**Abstract**

The present work explores the study of terahertz (THz) wave generation by the cross-focusing of two Gaussian laser beams in a bulk medium containing graphite nanoparticles (NPs). This system acts as a nonlinear medium behaving like plasma. The ripple is applied on the density of NPs to increase the conversion efficiency. Using the perturbative technique, a wave equation is derived which describes the nonlinear interaction of the laser beam with NPs. The nonlinear current at THz frequency arises due to the ponderomotive force exerted on the electrons of graphite NPs by the incident laser beams in the presence of density ripple. This nonlinearity depends on the intensities of both the beams. Hence the focusing of one beam affects the focusing of the other, resulting in the cross-focusing of the beams. Numerical results show that the normalized amplitude of the generated THz wave increases by 3.5 times with the consideration of the phenomenon of cross-focusing. The results show the enhancement in the efficiency of generated THz wave on application of density ripple, due to the fulfillment of the phase matching condition.

Keywords: THz radiation, nanoparticles, density ripple, cross-focusing

(Some figures may appear in colour only in the online journal)

## 1. Introduction

In the past few decades, investigations related to the synthesis of the nanoparticles (NPs) and study of their properties have become an active area of interest in different scientific areas like nano-optics, nanoelectronics, telecommunications, plasmonics etc [1–3]. It has been seen that, when the high power laser interacts with graphite NPs, ionization of NPs takes place due to the significant absorption of laser energy leading to the formation of high-temperature micro plasmas. In this medium, all free electrons undergo collective oscillations and make it to show the very high nonlinearity near the plasmon frequency. Thus, the efficiency of generated radiation or energetic particles in a medium containing NPs is very high compared to solid plasma.

Over the last two decades, the terahertz region of the electromagnetic radiation spectrum has been explored by various researchers. THz radiation sources have extensive applications in the field of remote sensing, short distance wireless communications, biological and chemical imaging, non destructive testing, high field condensed-matter studies and explosives detections etc [4–7]. A variety of schemes have been proposed to produce THz radiations [8–10]. As we know, plasma is capable of dealing with the high power laser and of generation of THz radiation with a high electric field without any physical damage to the medium. So, there are a number of mechanisms based on laser-plasma interaction with which high powered THz sources can be generated. In a report of Wu *et al* [11], we can observe the phenomenon of generation of THz radiations by a plasma filament created by short, intense laser pulse. Ladouceur *et al* [12] have reported a study of the generation of broadband THz within the plasma filaments on account of the short intense pulsed laser. Kumar *et al* [13] have studied the effect of self-focusing on the THz

 

radiation generation by considering the propagation of amplitude-modulated Gaussian laser beam in rippled density plasma. They observed that plasma density ripple provides the sufficient phase matching condition and plays a key role in the generation of THz radiation. Sharma and Singh [14] have investigated the effect of an external static electric field on THz radiation generation and concluded that the amplitude and power of the THz radiations increase with the increase in the amplitude of the static electric field.

Generation of twisted THz radiation by the interaction of the laser beam with plasma has been done by Sobhani and his group [15–18]. In their recent study they have proposed the generation of twisted THz radiation by the interaction of a laser beam with helical rippled density plasma [15]. They observed that when an intense laser propagates in plasma, the ponderomotive force pushes the electrons out of the region of high intensity. So a nonlinear interaction between laser and plasma vortex is produced, which generates a nonlinear current at the beating frequency of laser and plasma wave. In another study, Sobhani *et al* [16] have investigated the resonant vortex THz beam generation by the cross-focusing of two twisted coaxial laser beams. In order to satisfy the phase matching condition for the resonant excitation of terahertz radiation, the rippled density amplitude and the ripple wave number were suitably chosen. Various laser and plasma parameters were employed to yield vortex terahertz radiation with higher efficiency. Further, a new scheme to create a twisted terahertz wave in a static plasma vortex has been proposed [17], in which a static plasma vortex with a helical structure, submerged in the static electric field was taken. The torsion of the emitted THz radiation is provoked by the charge numbers of the lasers or the helical structure of static plasma vortex.

In the present analysis, we propose a model for the THz radiation generation by the beating of two Gaussian laser beams in a bulk medium consisting of graphite NPs under the influence of density ripple of NPs. The use of NPs as the THz radiation source is very effective due to their nanoscale dimensions and high conversion efficiency as explained earlier. The incident laser beams have non-uniform transverse spatial profile; hence the redistribution of charge carriers occurs leading to the cross-focusing of laser beams. Since, self-focusing of the laser beam in periodically arranged NPs have a number of practical applications [19, 20]. So it would be interesting to observe the effect of self-focusing of the incident laser beams on THz generation process in NPs. Hence, our goal is two fold: (1) to study the effect of density ripple amplitude on THz radiation generation, (2) to explore the effect of cross-focusing of laser beams on the THz generation efficiency. The lasers field exert ponderomotive force on the free electrons of graphite NPs generating a nonlinear velocity. This oscillatory velocity couples with density gradient to generate a macroscopic electron current at the beat frequency $(\omega_2 - 2\omega_1)$, which generates THz radiation. The interesting property of NPs is that, the optical properties of graphite NPs can be varied by changing the orientation of the electric field of the incident beam with respect to the basal-plane of NPs. Section 2 of the present work includes the theoretical considerations of nonlinear current density. Section 3 gives the formalism of THz radiation generation. Observations are discussed in section 4 and in the last section the present scheme is concluded.

## 2. Theoretical consideration

Consider the propagation of two intense laser beams $(\omega_1, \ \vec{k}_1)$ and $(\omega_2, \ \vec{k}_2)$ polarized in the $x$ direction and propagating along the $z$ direction in the bulk medium of graphite NPs. The periodic array of NPs is generated with an average particle radius $r_c$, average separation between particles $d$ and the density of the conduction electrons of NPs $n_0$. The macroscopic density of NPs is modulated using a structured nozzle [21]. The homogenous nucleation with subsequent condensation and agglomeration of the stream of noble gas coming out of this nozzle produces graphite NPs of rippled density as $n = n_q \exp(\mathrm{i}k_o z)$, where $n_q$ is the initial ripple density of NPs and $k_o$ is the ripple wave number.

In graphite there are four valence electrons per atom and four atoms per unit cell which are regularly located on equidistant planes called basal planes. It is considered that, the medium of our model contains two types of graphite NPs having parallel or perpendicular orientation of the electric field with respect to the graphite basal plane. The total macroscopic density of all NPs is $n = \sum_\alpha 4\pi l_\alpha n_{0,\alpha}/3$, where $\alpha = \perp, \ ||$ indicates the cases when an electric field vector is perpendicular and parallel to the unit vector normal to the basal plane, respectively. Here, $l_\alpha = (r_{c\alpha}/d_\alpha)^3$, $r_{c\alpha}$ and $d_\alpha$ are the average particle radius and average particle separation of $\alpha$ configured NPs, respectively.

The electric and magnetic fields of the laser beams can be represented as

$$\vec{E}_j = \hat{x} A_j \mathrm{e}^{-\mathrm{i}(\omega_j t - k_j z)}, \tag{1a}$$

$$\vec{B}_j = \frac{(\vec{k}_j \times \vec{E}_j)}{\omega_j}, \tag{1b}$$

where $A_j = (A_{0j}/f_j)\mathrm{e}^{-r^2/2r_{0j}^2 f_j^2}$ is the amplitude of the laser, $f_j$ is the beam width parameter, $r_{0j}$ is the initial beam radius, $k_j$ is the propagation constant and $j = 1, 2$.

The propagation constant $k_j$ can be derived from dispersion relation [22] as

$$k_j = \frac{\omega_j}{c}\left[\varepsilon_{\mathrm{eff}} - \sum \frac{4\pi}{3} l_\alpha \frac{\omega_{p\alpha}^2}{\omega_j^2 + \mathrm{i}\Gamma\omega_j - \omega_{p\alpha}^2/3}\right]^{1/2}, \tag{2}$$

where $\varepsilon_{\mathrm{eff}}$ is the effective electric permittivity of the medium, whose real and imaginary parts respectively can be written as [22]

$$\varepsilon_{\mathrm{effr}} = 1 - \frac{4\pi l_\alpha \omega_{p\alpha}^2(\omega^2 - \omega_{p\alpha}^2/3)}{3(\omega^2 - \omega_{p\alpha}^2/3)^2 + \omega^2\Gamma^2},$$

$$\varepsilon_{\mathrm{effi}} = \frac{4\pi l_\alpha \omega_{p\alpha}^2 \omega\Gamma}{3(\omega^2 - \omega_{p\alpha}^2/3)^2 + \omega^2\Gamma^2}.$$

Here, $\Gamma$ is the damping factor related to the electron scattering, $\omega_p = \sqrt{4\pi n_0 e^2/m}$ is the plasma frequency, $m$ and $e$ are

electronic mass and charge, respectively. Due to the presence of damping factor, $k_j$ will be imaginary, which leads to the absorption of waves.

We assume that, in the interaction of high frequency laser beams, only the spherical electronic cloud of NPs displaces through distance $x$ with respect to immobile ions. The restoration force due to this displacement is $-4\pi n_o e^2 x/3$. Hence, the equation of motion of an electron in the electron cloud of NPs is [22]

$$m\frac{\mathrm{d}\vec{v}_j}{\mathrm{d}t} = -e\vec{E}_j - \frac{m\omega_p^2}{3}\vec{x} - \Gamma m\vec{v}_j. \tag{3}$$

Solving this equation of motion, the oscillatory velocity acquired by an electron can be derived as

$$\vec{v}_j = -\frac{\mathrm{i}\omega_j e\vec{E}_j}{m[\omega_j^2 + \mathrm{i}\Gamma\omega_j - \omega_p^2/3]}. \tag{4}$$

Due to this oscillatory velocity, laser exerts ponderomotive force on electrons of NPs at $(\omega_2 - \omega_1)$ and $2\omega_1$ respectively as

$$\vec{F}_{p_{(\omega_2-\omega_1)}} = \frac{-m}{2}\vec{\nabla}(\vec{v}_1.\vec{v}_2^*)$$

$$= \frac{-\omega_1\omega_2 e^2 \mathrm{i}(k_1 - k_2)E_1E_2^*\hat{z}}{2m[\omega_1^2 + \mathrm{i}\Gamma\omega_1 - \omega_p^2/3][\omega_2^2 - \mathrm{i}\Gamma\omega_2 - \omega_p^2/3]}, \tag{5a}$$

$$\vec{F}_{p_{(2\omega_1)}} = \frac{-e}{2}(\vec{v}_1 \times \vec{B}_1) = \frac{\mathrm{i}e^2 k_1 E_1^2\hat{z}}{2m[\omega_1^2 + \mathrm{i}\Gamma\omega_1 - \omega_p^2/3]}. \tag{5b}$$

The oscillatory velocities of the electrons of NPs due to these forces can be derived as

$$\vec{v}^{NL}_{(\omega_2-\omega_1)} = -\frac{(\omega_2 - \omega_1)\vec{F}_{p(\omega_2-\omega_1)}}{m\mathrm{i}[(\omega_2 - \omega_1)^2 + \mathrm{i}\Gamma(\omega_2 - \omega_1) - \omega_p^2/3]}, \tag{6a}$$

$$\vec{v}^{NL}_{2\omega_1} = -\frac{-2\omega_1\vec{F}_{p(2\omega_1)}}{m\mathrm{i}[4\omega_1^2 + 2\mathrm{i}\Gamma\omega_1 - \omega_p^2/3]}. \tag{6b}$$

These velocities give rise to density oscillations at $(\omega_2 - \omega_1,\ \ k_2 - k_1)$ and $(2\omega_1,\ \ 2k_1)$ which can be derived using an equation of continuity as

$$n^{NL}_{(\omega_2-\omega_1)} = \frac{-n_0\vec{F}_{p(\omega_2-\omega_1)}(k_2 - k_1)}{m\mathrm{i}[(\omega_2 - \omega_1)^2 + \mathrm{i}\Gamma(\omega_2 - \omega_1) - \omega_p^2/3]}, \tag{7a}$$

$$n^{NL}_{2\omega_1} = \frac{-n_0\vec{F}_{p(2\omega_1)}2k_1}{m\mathrm{i}[4\omega_1^2 + 2\mathrm{i}\Gamma\omega_1 - \omega_p^2/3]}. \tag{7b}$$

These nonlinear density perturbations at $(\omega_2 - \omega_1,\ k_2 - k_1)$ produce a self-consistent space charge electrostatic potential $\Phi_s = \Phi_{so}\mathrm{e}^{-\mathrm{i}[(\omega_2-\omega_1)t - \mathrm{i}(k_2-k_1)z]}$ and hence, electrostatic field $\vec{E}_s = -\vec{\nabla}\Phi_s$. This field perturbs the electron density of NPs linearly as

$$n^L_{(\omega_2-\omega_1)} = \frac{(k_2 - k_1)^2\chi\Phi_s}{4\pi e}, \tag{8}$$

where, $\chi = -\omega_p^2/[(\omega_2 - \omega_1)^2 + \mathrm{i}\Gamma(\omega_2 - \omega_1) - \omega_p^2/3]$ is the susceptibility of the electrons of NPs. From Poisson's equation, we can derive

$$\Phi_s = \frac{-4\pi e n^{NL}_{(\omega_2-\omega_1)}}{(1 + \chi)(k_2 - k_1)^2}. \tag{9}$$

Putting equation (9) in (8) we get

$$n^L_{(\omega_2-\omega_1)} = \frac{-n^{NL}_{(\omega_2-\omega_1)}\chi}{(1 + \chi)}. \tag{10}$$

Hence, total density perturbations at $(\omega_2 - \omega_1,\ \ k_2 - k_1)$ is

$$n_{(\omega_2-\omega_1)} = \frac{n^{NL}_{(\omega_2-\omega_1)}}{(1 + \chi)}. \tag{11}$$

Similarly, at $(2\omega_1,\ \ 2k_1)$

$$n^L_{(2\omega_1)} = \frac{4k_1^2\chi'\Phi_s'}{4\pi e}, \tag{12}$$

where $\chi' = -\omega_p^2/[4\omega_1^2 + 2\mathrm{i}\Gamma\omega_1 - \omega_p^2/3]$ and

$$\Phi_s' = \frac{-4\pi e n^{NL}_{(2\omega_1)}}{(1 + \chi')4k_1^2}. \tag{13}$$

The total density perturbation at $(2\omega_1,\ \ 2k_1)$ is

$$n_{(2\omega_1)} = \frac{n^{NL}_{(2\omega_1)}}{1 + \chi'}. \tag{14}$$

The nonlinear current density at THz frequency $\omega = \omega_2 - 2\omega_1$ and $k = k_2 - 2k_1 + k_o$ is

$$\vec{J}^{NL}_{\omega} = -\frac{e}{2}n^*_{(\omega_2-\omega_1)}\vec{v}^*_{\omega_1} - \frac{e}{2}n^*_{(2\omega_1)}\vec{v}_{\omega 2}$$

$$= -\frac{\mathrm{i}(k_2 - k_1)^2 n_0 e^4 {E_1^*}^2 E_2\omega_1^2\omega_2\hat{z}}{(1 + \chi^*)4m^3[\omega_1^2 - \mathrm{i}\Gamma\omega_1 - \omega_p^2/3][(\omega_2 - \omega_1)^2 - \mathrm{i}\Gamma(\omega_2 - \omega_1) - \omega_p^2/3][\omega_2^2 + \mathrm{i}\Gamma\omega_2 - \omega_p^2/3]}$$

$$-\frac{\mathrm{i}k_1^2 n_0 e^4 {E_1^*}^2 E_2\omega_2\hat{z}}{(1 + \chi'^*)2m^3[4\omega_1^2 - 2\mathrm{i}\Gamma\omega_1 - \omega_p^2/3][\omega_1^2 - \mathrm{i}\Gamma\omega_1 - \omega_p^2/3][\omega_2^2 + \mathrm{i}\Gamma\omega_2 - \omega_p^2/3]}. \tag{15}$$

Total nonlinear macroscopic current density because of the whole system is

$$(\vec{J}_{av}^{NL})_{\text{Tot}} = \sum 4\pi l_\alpha \vec{J}_{\omega,\alpha}^{NL}/3$$
$$= \sum -\left( \frac{\mathrm{i}(k_2-k_1)^2 e^2 \omega_1^2 \omega_2}{(1+\chi'^*)12m^2} \frac{n_{q0}}{n_0} \frac{\omega_{p,\alpha}^2 l_\alpha A_1^{*^2} A_2}{[\omega_1^2 - \mathrm{i}\Gamma_\alpha\omega_1 - \omega_{p,\alpha}^2/3]^2 [\omega_2^2 + \mathrm{i}\Gamma_\alpha\omega_2 - \omega_{p,\alpha}^2/3][(\omega_2-\omega_1)^2 - \mathrm{i}\Gamma_\alpha(\omega_2-\omega_1) - \omega_{p,\alpha}^2/3]} \right.$$
$$\left. + \frac{\mathrm{i}k_1^2 e^2 \omega_2}{(1+\chi'^*)6m^2} \frac{n_{q0}}{n_0} \frac{\omega_{p,\alpha}^2 l_\alpha A_1^{*^2} A_2}{[4\omega_1^2 - 2\mathrm{i}\Gamma_\alpha\omega_1 - \omega_{p,\alpha}^2/3][\omega_1^2 - \mathrm{i}\Gamma_\alpha\omega_1 - \omega_{p,\alpha}^2/3][\omega_2^2 + \mathrm{i}\Gamma_\alpha\omega_2 - \omega_{p,\alpha}^2/3]} \right) \mathrm{e}^{-\mathrm{i}[(\omega_2-2\omega_1)t-(k_2-2k_1+k_0)z]}. \quad (16)$$

We can write the linear current density of system of NPs at $(\omega, \quad k)$ as

$$(\vec{J}_{av}^{L})_{\text{Tot}} = \sum \frac{4\pi}{3} l_\alpha \left( \frac{-n_0 e^2 \vec{E}_\omega}{m\mathrm{i}\omega} \right). \quad (17)$$

## 3. Formalism of terahertz generation

For the initial transverse intensity profile of the incident laser beams, the radial gradient of refractive index of the medium is created. This results in the focusing of the beams in the medium, where the convergence of light takes place macroscopically in the region of interaction. Using paraxial ray & WKB approximation, the coupled cross-focusing equations for two incident laser beams, governing the dimensionless beam width parameters in above described collisionless plasma can be derived as [23, 24]

$$\frac{\partial^2 f_j}{\partial z^2} = \frac{1}{k_j^2 r_{0j}^4 f_j^3} - \frac{f_j}{2\varepsilon_{0j}} \left( \frac{\omega_p}{\omega_j} \right)^2 \left( \frac{\alpha_1 E_{01}^2}{f_1^4 r_{01}^2} + \frac{\alpha_2 E_{02}^2}{f_2^4 r_{02}^2} \right) \times \exp\left( -\frac{\alpha_1 E_{01}^2}{f_1^2} - \frac{\alpha_2 E_{02}^2}{f_2^2} \right), \quad (18)$$

where, $\alpha_j = e^2/8m\omega_j^2 k_B T$, $\varepsilon_{0j} = 1 - \omega_p^2/\omega_j^2$.

The THz wave propagation equation can be written as

$$\nabla^2 \vec{E}_\omega - \vec{\nabla}(\vec{\nabla}.\vec{E}_\omega) = \frac{4\pi}{c^2} \frac{\partial[(\vec{J}_{av}^{NL})_{\text{Tot}} + (\vec{J}_{av}^{L})_{\text{Tot}}]}{\partial t} + \frac{\varepsilon_{\text{eff}}}{c^2} \frac{\partial^2 \vec{E}_\omega}{\partial t^2} \quad (19)$$

Here, $\vec{E}_\omega$ is THz field which varies as $\vec{E}_\omega = \hat{x} A_\omega(z, t)\mathrm{e}^{-\mathrm{i}(\omega t - kz)}$.

Neglecting $\vec{\nabla}(\vec{\nabla}.\vec{E}_\omega)$, which is valid almost for all practical situations, equation (19) can be written as

$$2\mathrm{i}k \frac{\partial A_\omega}{\partial z} - k^2 A_\omega - \frac{\omega_{p,\alpha}^2}{c^2} \frac{4\pi l_\alpha A_\omega}{3} + \frac{\varepsilon_{\text{eff}} \omega^2 A_\omega}{c^2} = -\frac{4\pi \mathrm{i}\omega\omega_1}{c^2} \frac{A_{01} \mathrm{e}^{-r^2/r_{01}^2 f_1^2} \mathrm{e}^{-r^2/2r_{02}^2 f_2^2} Q_\alpha}{f_1^2 f_2}, \quad (20)$$

where

$$Q_\alpha = -\sum \left( \frac{\mathrm{i}k_1^2 c^2 a_1 a_2}{12\omega_1^2(1+\chi^*)} \left( \frac{k_2}{k_1} - 1 \right)^2 \frac{n_{q0}}{n_0} \frac{\omega_{p,\alpha}^2}{\omega_1^2} \frac{l_\alpha}{\left[ \left( \frac{\omega_2}{\omega_1} - 1 \right)^2 - \frac{\mathrm{i}\Gamma_\alpha}{\omega_1} \left( \frac{\omega_2}{\omega_1} - 1 \right) - \frac{\omega_{p,\alpha}^2}{3\omega_1^2} \right] \left[ 1 - \frac{\mathrm{i}\Gamma_\alpha}{\omega_1} - \frac{\omega_{p,\alpha}^2}{3\omega_1^2} \right]^2 \left[ 1 + \frac{\mathrm{i}\Gamma_\alpha}{\omega_2} - \frac{\omega_{p,\alpha}^2}{3\omega_2^2} \right]} \right.$$
$$\left. + \frac{\mathrm{i}k_1^2 c^2 a_1 a_2}{6\omega_1^2(1+\chi'^*)} \frac{n_{q0}}{n_0} \frac{\omega_{p,\alpha}^2}{\omega_1^2} \frac{l_\alpha}{\left[ 4 - \frac{2\mathrm{i}\Gamma_\alpha}{\omega_1} - \frac{\omega_{p,\alpha}^2}{3\omega_1^2} \right] \left[ 1 - \frac{\mathrm{i}\Gamma_\alpha}{\omega_1} - \frac{\omega_{p,\alpha}^2}{3\omega_1^2} \right]^2 \left[ 1 + \frac{\mathrm{i}\Gamma_\alpha}{\omega_2} - \frac{\omega_{p,\alpha}^2}{3\omega_2^2} \right]} \right), \quad (21)$$

$a_1 = eA_{01}/m\omega_1 c$ and $a_2 = eA_{02}/m\omega_2 c$. On simplification, equation (20) can be written as

$$\frac{\partial A_\omega}{\partial z} + k' A_\omega = \frac{-2\pi\omega\omega_1}{kc^2} Q_\alpha \frac{A_{01}^2}{f_1^2 f_2} \mathrm{e}^{-\frac{r^2}{r_{01}^2 f_1^2}} \mathrm{e}^{-\frac{r^2}{2r_{02}^2 f_2^2}}, \quad (22)$$

where $k' = (\varepsilon_{\text{eff}}\omega^2 - \omega_p^2 4\pi l_\alpha/3 - k^2c^2)/(2\mathrm{i}kc^2)$.

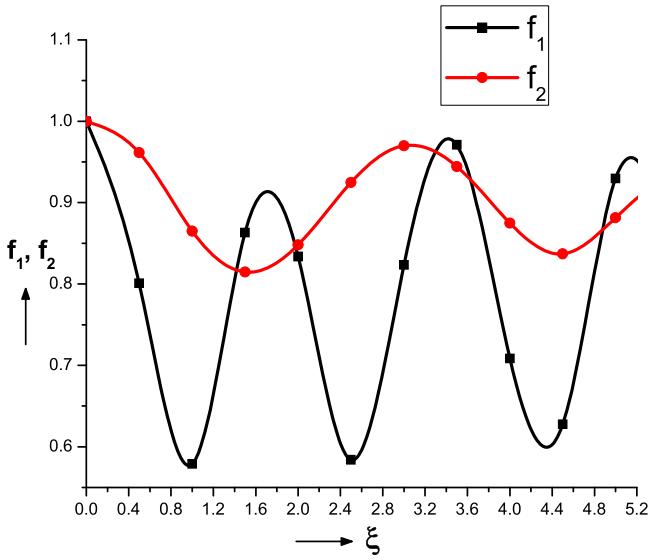


**Figure 1.** Variation of beam width parameters $f_1$ and $f_2$ with normalized distance of propagation $\xi$ at $\alpha_1 A_{01}^2 = 0.6$, $\alpha_2 A_{02}^2 = 0.4$ and $n_{q0}/n_0 = 0.5$.

Defining dimensionless distance of propagation $\xi$ as $\xi = z/(k_1 r_{01}^2)$, the equation for THz wave amplitude can be written as

$$\frac{\partial}{\partial \xi}\left(\frac{A_\omega}{A_{01}}\right) + k_1 r_{01}^2 k'\left(\frac{A_\omega}{A_{01}}\right) = \frac{-2\pi\omega\omega_1 r_{01}^2}{c^2} Q_\alpha \frac{k_1}{k}\frac{1}{f_1^2 f_2^2} e^{-\frac{r^2}{r_{01}^2 f_1^2}} e^{-\frac{r^2}{2r_{02}^2 f_2^2}}. \quad (23)$$

Also, in terms of dimensionless parameter $\xi$, equation (18) can be written as

$$\frac{\partial^2 f_1}{\partial \xi^2} = \frac{1}{f_1^3} - \left(\frac{\omega_p r_{01}}{c}\right)^2 \frac{f_1}{2}\left[\frac{\alpha_1 E_{01}^2}{f_1^4} + \frac{\alpha_2 E_{02}^2}{f_2^4}\left(\frac{r_{01}}{r_{02}}\right)^2\right] \times \exp\left(-\frac{\alpha_1 E_{01}^2}{f_1^2} - \frac{\alpha_2 E_{02}^2}{f_2^2}\right), \quad (24)$$

$$\frac{\partial^2 f_2}{\partial \xi^2} = \frac{1}{f_2^3} - \left(\frac{\omega_p r_{01}}{c}\right)^2 \left(\frac{\varepsilon_{01}}{\varepsilon_{02}}\right)\left(\frac{\omega_1}{\omega_2}\right)\left(\frac{f_2}{2}\right) \times \left(\frac{\alpha_1 E_{01}^2}{f_1^4} + \frac{\alpha_2 E_{02}^2}{f_2^4}\left(\frac{r_{01}}{r_{02}}\right)^2\right) \exp\left(-\frac{\alpha_1 E_{01}^2}{f_1^2} - \frac{\alpha_2 E_{02}^2}{f_2^2}\right). \quad (25)$$

## 4. Observations and discussion

To draw the inferences from the above equations, these are solved numerically using the following set of laser, plasma and NPs parameters: $CO_2$ laser of frequencies $\omega_1 = 2 \times 10^{14}$ rad s$^{-1}$ and $\omega_2 = 4.2 \times 10^{14}$ rad s$^{-1}$ are chosen such that difference $\omega_2 - 2\omega_1$ lies in THz range. The plasma frequency $\omega_p$ is $1.78 \times 10^{13}$ rad s$^{-1}$. Corresponding to above mentioned frequencies of lasers, the wavelengths are $\lambda_1 = 10.2$ $\mu$m, $\lambda_2 = 9.44$ $\mu$m with peak intensities $I \approx 10^{16}$ W cm$^{-2}$, initial spot sizes $r_{01} = 50$ $\mu$m and $r_{02} = 30$ $\mu$m. The separation between NPs is considered to be twice of their radius. The radius and separation between particles for both the morphologies are considered to be same, i.e. $r_{c\parallel} = r_{c\perp}$ and $d_\parallel = d_\perp$.

Equations (24), (25) are the cross-focusing equations of the laser beams in the nonlinear bulk medium containing graphite NPs. The first term on the right-hand side of these equations is the diffraction term, responsible for the divergence of the beams. The second term arises due to the nonlinearity of the medium and is responsible for the convergence of the beams. Equations (23)–(25) are the coupled equations and the results obtained by solving them are presented in the form of 3D plots. Figure 1 shows the variation of beam width parameters $f_1$ and $f_2$ of two laser beams with a normalized distance of propagation $\xi$ at laser beams intensities $\alpha_1 A_{01}^2 = 0.6$ and $\alpha_2 A_{02}^2 = 0.4$ (corresponding $a_1 = 1.2$ and $a_2 = 1$). The nonuniform transverse intensity profiles of incident Gaussian beams produce radial refractive index gradient which results in the focusing of the beams. The propagation of one beam in the medium depends not only upon its own intensity but the intensity of the other beam as well. During the simultaneous propagation of two Gaussian beams, the focusing of the first beam is governed by the second and vice versa. Hence, because of the mutual interaction of the two Gaussian laser beams, the cross-focusing of both beams occurs in the plasma. This phenomenon of cross-focusing of two beams is shown in figure 1.

Figures 2(a) and (b) show the 3D variation of the normalized THz wave amplitude in the radial ($r/r_{01}$) and axial direction ($\xi = z/k_1 r_{01}^2$) at $n_q = 0.5$, without (i.e. $f_1 = f_2 = 1$) and with cross- focusing, respectively. One can observe from this figure that, the amplitude of generated THz beam is maximum along the axis of the co-propagating laser beams and it decreases with increasing the radial distance $r/r_{01}$. In the axial direction, THz amplitude shows an oscillatory behavior and exhibits maxima and minima with the distance of propagation $\xi$. It is clear from figure 2 that the amplitude of THz wave increases by 3.5 times with cross- focusing in comparison of without cross focusing. The physical mechanism for this result can be explained as follows: with the focusing of the beam, the intensity of the beam increases which leads to an increase in the THz amplitude. Such amplitude enhancement in THz generation in the presence of cross-focusing has also been observed by Sharma and Singh [14] in collisional plasma. In figure 2(b), the third peak at distance $\xi = 4.4$ is observed to have a maximum amplitude in compared to the other two peaks. At $\xi = 4.4$, both the beams are focused (can be observed from figure 1), because of which their intensities increase and the simultaneous increase of intensity of both the beams affects the amplitude of generated THz wave, resulting in its enhancement.

In figure 3(b), the variation of the normalized THz amplitude $A_\omega/A_{01}$ with $r$ and $\xi$ (with which the laser beams show oscillatory focusing) is shown in the presence of cross-focusing phenomenon at laser beam intensities $\alpha_1 A_{01}^2 = 0.3$ and $\alpha_2 A_{02}^2 = 0.3$ (corresponding $a_1 = 1.2$ and $a_2 = 1$). Here, the axial distance of propagation at which one gets the highest

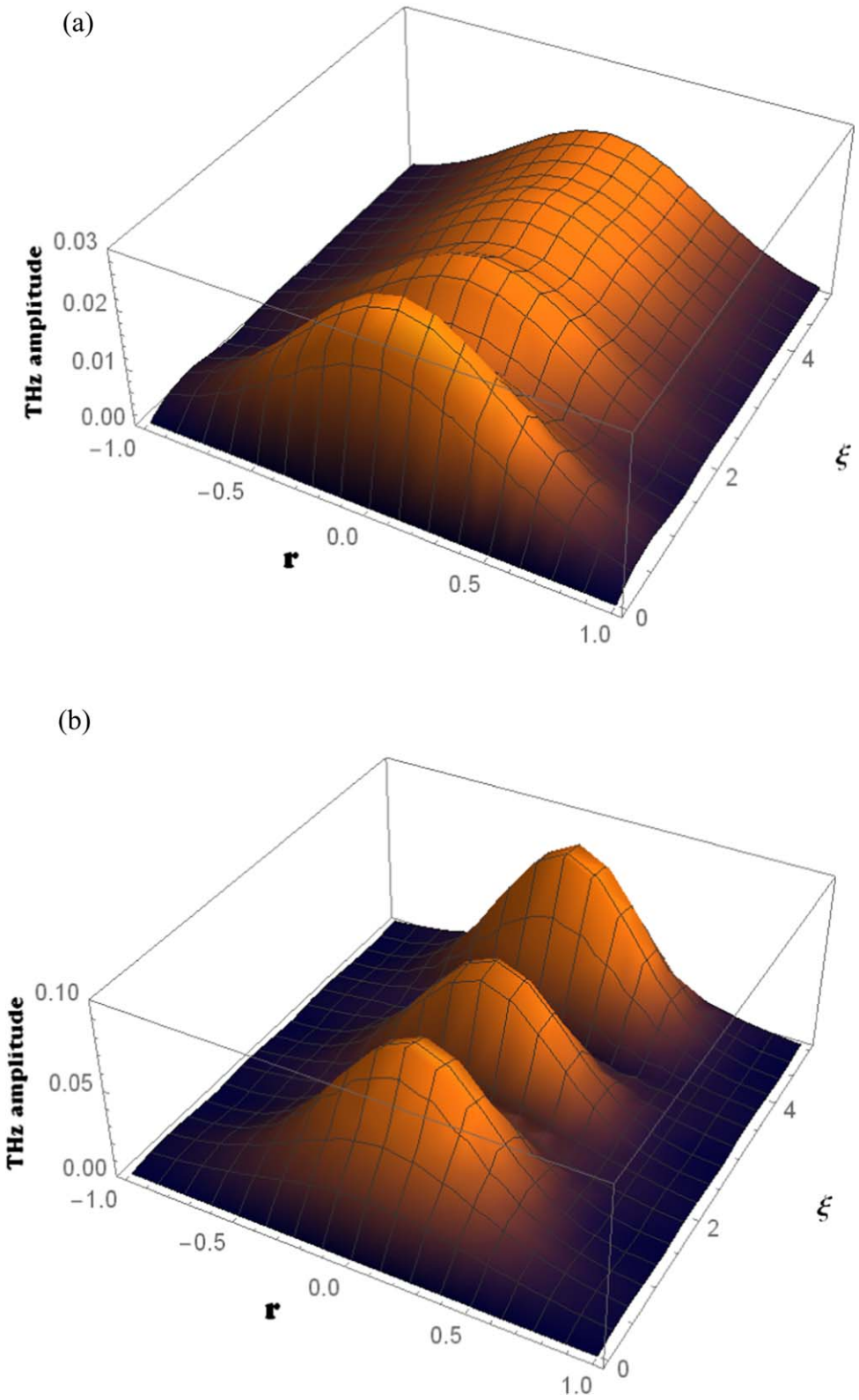


**Figure 2.** Variation of the normalized THz amplitude $A_\omega/A_{01}$ with $r$ and $\xi$ (a) without cross-focusing (b) with cross-focusing at $n_{q0}/n_0 = 0.5$, $\alpha_1 A_{01}^2 = 0.6$ and $\alpha_2 A_{02}^2 = 0.4$.

THz amplitude is altered. Now the THz amplitude enhancement occurs at $\xi = 1.1$ and $\xi = 4.1$. These are those distances where both the beams are focused (figure 3(a)). Hence, the focusing of the laser beams in NPs plays a significant role in the conversion mechanism. These results are in accordance with the results of Sharma *et al* [25], who have studied the effect of focusing mechanism on THz radiation generation in collisionless magnetoplasma in the presence of density ripple.

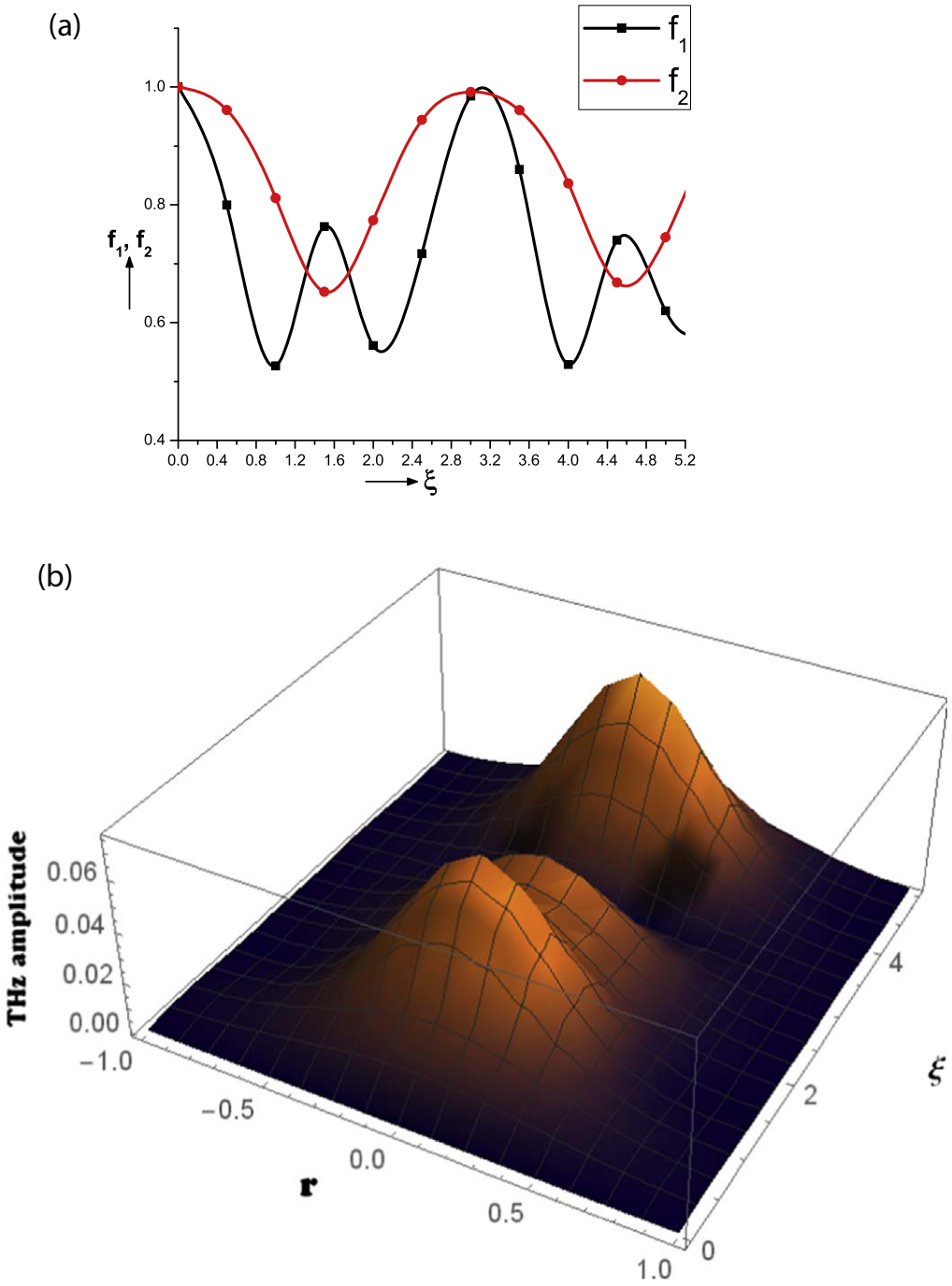


**Figure 3.** (a) Variation of beam width parameters $f_1$ and $f_2$ with normalized distance of propagation $\xi$ at $\alpha_1 A_{01}^2 = 0.3$, $\alpha_2 A_{02}^2 = 0.3$ and $n_{q0}/n_0 = 0.5$. (b) Variation of the normalized THz amplitude $A_\omega/A_{01}$ with $r$ and $\xi$ with cross-focusing at $n_{q0}/n_0 = 0.5$, $\alpha_1 A_{01}^2 = 0.3$ and $\alpha_2 A_{02}^2 = 0.3$.

The effect of density ripple of NPs on the THz amplitude of the laser beam is shown in figure 4. It shows the variation of normalized THz wave amplitude against the normalized ripple amplitude $n_{q0}/n_0$ and $\xi$ at $r = 0$ with cross focusing phenomenon. Here, the amplitude of THz wave increases with the increase of ripple amplitude. This is because, with the increase of ripple amplitude, the electron density involved in the generation of nonlinear current at THz frequency increases and hence, the THz amplitude increases. Qualitatively, this observation is in accordance with the study reported by Bhasin *et al* [26] who have showed that the THz power scales as the square of density ripple amplitude in a rippled density magnetized plasma.

Actually, the wave vector $k$ of the generated THz wave increases more than the wave vector corresponding to the beating of two waves, i.e. $k_2 - 2k_1$. Hence the momentum of the system is not conserved. To conserve the momentum, the additional momentum is provided by density ripple, which

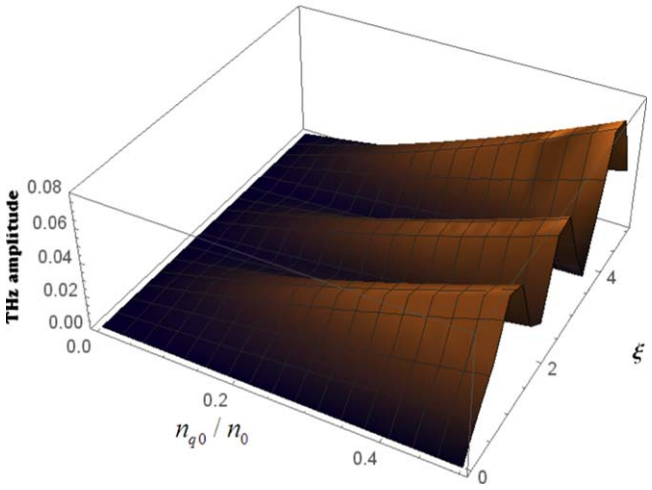


**Figure 4.** Variation of the normalized THz amplitude $A_\omega/A_{01}$ with $n_{q0}/n_0$ and $\xi$ with cross-focusing at $r = 0$, $\alpha_1 A_{01}^2 = 0.6$ and $\alpha_2 A_{02}^2 = 0.4$.

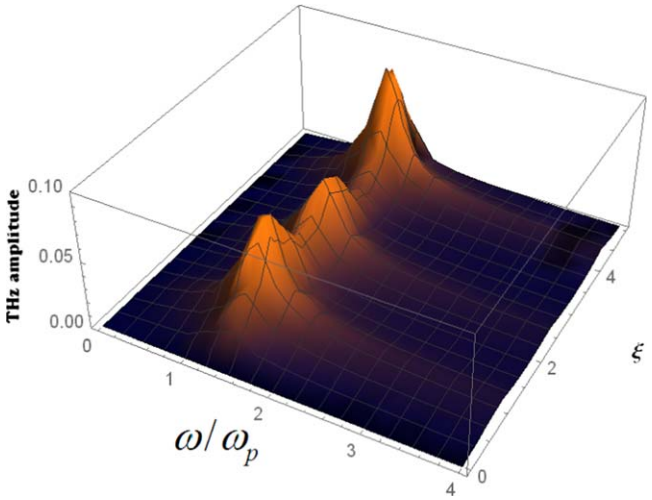


**Figure 5.** Variation of the normalized THz amplitude $A_\omega/A_{01}$ with $\omega/\omega_p$ and $\xi$ with cross-focusing at $r = 0$, $n_{q0}/n_0 = 0.5$, $\alpha_1 A_{01}^2 = 0.6$ and $\alpha_2 A_{02}^2 = 0.4$.

helps to satisfy the phase matching condition. The requisite ripple wave number for resonant THz generation is

$$k_o = k - k_2 + 2k_1 = \frac{\omega}{c}\left[1 - \left(\varepsilon_{\text{eff}} - \sum \frac{4\pi}{3} l_\alpha \frac{\omega_{p\alpha}^2}{\omega^2 + i\Gamma\omega - \omega_{p\alpha}^2/3}\right)^{1/2}\right].$$

Hence, the purpose of applying the density ripple is to provide a suitable phase for efficient THz radiation. Hence, the increase in density modulation of NPs enhances the THz amplitude.

Figure 5 depicts the variation of the normalized THz amplitude $A_\omega/A_{01}$ with the beat frequency $\omega/\omega_p$ and $\xi$ with the cross-focusing phenomenon at $r = 0$. From this figure, it is observed that the THz field amplitude gets the maximum as the beating frequency $\omega$ approaches the plasma frequency $\omega_p$. This is because at this frequency resonance occurs and we obtain THz wave of highest amplitude. Hence, it can be concluded that the THz radiation of desirable amplitude can be generated in NPs by optimizing the value of ripple amplitude $n_{q0}/n_0$ on the density of NPs, distances of propagation $\xi$ and $r/r_{01}$, laser intensities $\alpha_1 A_{01}^2$, $\alpha_1 A_{02}^2$ and beat frequency $\omega$.

## 5. Conclusion

We study the effect of cross-focusing of two laser beams on THz wave generation in the interaction of the laser beam with bulk medium containing graphite NPs. Using paraxial ray and Wentzel–Kramers–Brillouin approximation, the nonlinear coupled differential equations governing the dynamics of beam width parameters of the laser beams have been derived. The nonlinearity arises due to ponderomotive force taken into consideration. This nonlinearity results in the cross-focusing of incident laser beams in the medium of periodically arranged NPs in a region with characteristic dimensions smaller than the incident wavelength. A significant magnitude enhancement in the amplitude of the generated THz wave is observed in the presence of a cross-focusing phenomenon, in contrast to the case in which it is absent. Further, the ripple in the density of NPs enhances the generation efficiency of THz wave by satisfying the phase matching condition. Thus, the efficiency of the THz wave generated in the proposed scheme can be potentially used in various applications in the field of nano-optics.

## ORCID iDs

Vishal Thakur https://orcid.org/0000-0002-5347-6956
Niti Kant https://orcid.org/0000-0002-0293-3483
Shivani Vij https://orcid.org/0000-0003-1875-580X

## References

[1] Baraton M I 2002 *Synthesis, Functionalization and Surface Treatment of Nanoparticles* (Los Angeles: American Scientific)
[2] Wang Q, Xu J and Xie R H 2004 *Encyclopedia of Nanoscience and Nanotechnology* 8 (Los Angeles: American Scientific) 101
[3] Wehrspohn R B, Kitzerow H-S and Busch K 2008 *Nanophotonic materials : photonic crystals, plasmonics, and metamaterials* Wiley-VCH , Weinheim
[4] Zhong H, Redo-Sanchez A and Zhang X C 2006 *Opt. Express* **14** 9130
[5] Orenstein J and Millis A J 2000 *Science* **288** 468
[6] Fitch M J and Osiander R 2004 *Johns Hopkins APL Tech. Dig.* **25** 348
[7] Shen Y C, Lo T, Taday P F, Cole B E, Tribe W R and Kemp M C 2005 *Appl. Phys. Lett.* **86** 241116
[8] Muggli P, Liou R, Lai C H, Hoffman J, Katsouleas T C and Joshi C 1998 *Phys. Plasmas* **5** 2112
[9] Kukushkin V A 2008 *Europhys. Lett.* **84** 60002
[10] Leemans W P, Tilborg J V, Faure J, Geddes C G R, Toth C, Schroeder CB, Esarey E, Fubiani G and Dugan G 2004 *Phys. Plasmas* **11** 2899–906

[11] Wu HC, Meyer-Ter-Vehn J, Ruhland H and Sheng ZM 2011 *Phys. Rev.* E **83** 036407
[12] Ladouceur H D, Baronnavski A P, Lohrmann D, Grounds P W and Girardi P G 2001 *Opt. Commun.* **189** 107–11
[13] Kumar S, Singh R K, Singh M and Sharma R P 2015 *Laser Part. Beams* **33** 257–63
[14] Sharma R P and Singh R K 2014 *Phys. Plasmas* **21** 073101
[15] Sobhani H, Rooholamininejad H and Bahrampour A 2016 *J. Phys. D: Appl. Phys.* **49** 295107
[16] Sobhani H, Vaziri M, Rooholamininejad H and Bahrampour A 2016 *Eur. Phys. J.* D **70** 168
[17] Sobhani H 2017 *EPL* **119** 15001
[18] Sobhani H, Dehghan M and Dadar E 2017 *Phys. Plasmas* **24** 023110
[19] Barsch N, Jakobi J, Weiler S and Barcikowski S 2009 *Nanotechnology* **20** 445603
[20] Ganeev RA, Ryasnyansky A I, Stepanov A L, Marques C, da Silva R C and Alves E 2005 *Opt. Commun.* **253** 205
[21] Khan I, Saeed K and Khan I 2017 *Arab. J. Chem.* **423** 1
[22] Javan N S, Erdi F R and Najafi M N 2017 *Phys. Plasmas* **24** 052301
[23] Sodha M S, Ghatak A K and Tripathi V K 1974 *Self-Focusing of Laser Beams in Dielectrics, Plasmas and Semiconductors* (Delhi: Tata-McGraw-Hill)
[24] Akhmanov S A, Sukhorukov A P and Khokhlov R V 1968 *Sov. Phys.—Usp.* **10** 609
[25] Sharma R P, Monika A, Sharma P, Chauhan P and Ji A 2010 *Laser Part. Beams* **28** 531
[26] Bhasin L and Tripathi V K 2009 *Phys. Plasmas* **16** 103105